Available online at www.sciencedirect.com
ScienceDirect
Polymer 48 (2007) 2064–2070
polymer
www.elsevier.com/locate/polymer

Structure of the spinning apparatus of a wild silkworm *Samia cynthia ricini* and molecular dynamics calculation on the structural change of the silk fibroin

Tetsuo Asakura [a,*], Juming Yao [b], Mingying Yang [a], Zhenghua Zhu [a], Haruko Hirose [c]

[a] *Department of Biotechnology, Tokyo University of Agriculture and Technology, Koganei, Tokyo 184-8588, Japan*
[b] *The Key Laboratory of Advanced Textile Materials and Manufacturing Technology of Ministry of Education, College of Materials and Textile, Zhejiang Sci-Tech University, Hangzhou 310018, China*
[c] *Material Analysis Research Laboratories, Teijin Ltd, Hino, Tokyo 191-8515, Japan*

Received 12 September 2006; received in revised form 25 January 2007; accepted 30 January 2007
Available online 8 February 2007

Abstract

Silkworms have been developed over thousands years to optimize folding and crystallization of fibroin under highly controlled conditions which have resulted in their efficient fiber formation. In this paper, we reconstructed the three-dimensional architecture of the spinneret of a wild silkworm *Samia cynthia ricini* from approximately 1000 optical micrographs of the semi-thin cross sections. The chitin plates and muscles were observed in the silk press part together with large change in the diameter of the spinneret lumen at the press part by large shear stress. This is similar to the case of the spinneret of *Bombyx mori* silkworm, indicating that the structural change in the silk fibroin of *S.c. ricini* silkworm occurs exclusively at the silk press part due to large shear stresses. Molecular dynamics (MD) calculations were then performed to study the structural change that occurs in the crystalline region of *S.c. ricini* silk fibroin under shear stress. Namely, using the peptide AGGAGG$(A)_{12}$-GGAGAG as a model of the crystalline part of the silk fibroin under different shear stresses in the presence of water molecules and followed by molecular mechanics (MM) calculation after removal of water molecules. The simulation indicates that the Ala residues in the model peptides adopt a predominantly β-sheet structure under shear stresses of above 1.0 GPa.

Keywords: *Samia cynthia ricini* silk fibroin; 3D architecture of spinneret; Molecular dynamics calculation

1. Introduction

Silk proteins are of practical interest because of their excellent intrinsic properties which can be utilized in the biotechnological and biomedical fields as well as the importance of silkworm silks in the manufacture of high-quality textiles [1–3]. On the other hand, moderate quantities of silks and silk-mimic biopolymers have been produced due to the advances in molecular biotechnology and protein engineering [4–6]. However, production of useful materials, such as fibers, from these potential supplies of unprocessed biopolymers requires a detailed understanding of the processing technology necessary to induce the hierarchical structure responsible for the outstanding mechanical properties exhibited by native fibers. So the final hurdle on the way to the production of man-made silks now lies in the development of an appropriate spinning technology capable of converting these raw materials into high-performance fibers.

Samia cynthia ricini (*S.c. ricini*) is a wild silkworm. The primary structure of *S.c. ricini* silk fibroin consists of repeated sequences, a polyalanine (PLA) region and a Gly-rich region [7]. This is similar to the primary structure of dragline silk from spider although the length of PLA is shorter than that of the dragline silk, i.e., $(Ala)_{5-6}$ in spider dragline silk, while it

* Corresponding author. Tel./fax: +81 42 383 7733.
E-mail address: asakura@cc.tuat.ac.jp (T. Asakura).

0032-3861/$ - see front matter © 2007 Elsevier Ltd. All rights reserved.
doi:10.1016/j.polymer.2007.01.071

is $(Ala)_{12-13}$ in *S.c. ricini* silk fibroin [8–10]. From solution ^{13}C and ^{15}N NMR studies of *S.c. ricini* silk fibroin in aqueous solution, it has been reported that approximately 70% of Ala residues are in α-helix form, while other Ala residues are in random coil state [11–13]. The fast-exchange in the NMR time scale between helix and coil forms of the PLA region has been observed during helix to coil transition with change in temperature [11]. However, most of the glycine residues keep a random coil conformation during the helix–coil transition of the PLA region [7]. On the other hand, in the *S.c. ricini* silk fibroin fiber, Ala residues were proposed to form predominantly anti-parallel β-sheet structure with significant amounts of other structure [14–16].

Similar to the *Bombyx mori* silk, the *S.c. ricini* silk filament emerging from the silkworm consists of two fibroin protein monofilaments enveloped in a proteinaceous sericin coat [17,18]. Both fibroin and sericin are produced by very large, flattened cells lining a pair of long tubular silk glands. The silk gland consists of three distinct successive parts; the thin and flexuous posterior part, the wider middle and anterior parts. The silk fibroins are synthesized in the posterior part of the silk gland, and then transported down the lumen into the middle part of the silk gland in which it is stored in a concentrated state as a weak gel before spinning. It has been pointed out that the silk press part is important in the process of fiber formation from the liquid silk fibroin [18,19].

Recently, the ^{13}C CP/MAS NMR spectroscopy has been used to clarify the detailed structure of *S.c. ricini* silk fibroin [15,16]. The broad and asymmetric Ala Cβ signal in the NMR spectrum suggested a heterogeneous structure in the *S.c. ricini* silk fibroin fibers. With a deconvolution process by assuming Gaussian lineshape, the Ala Cβ ^{13}C NMR signal yielded four isotropic peaks at 15.7, 17.5, 20.8 and 22.8 ppm, assigned to α-helix, random coil and two kinds of β-sheet structure, respectively. Moreover, resulting structural transition was monitored by ^{13}C NMR stretching the *S.c. ricini* silk fibroin film prepared with aqueous silk solution extracted from the silk glands. The data indicated that the silk film underwent a structural transition from α-helix to β-sheet by increasing the stretching ratio. Remarkably the structural transition occurred when the stretching ratio was between ×4 and ×6. A broad and asymmetric Ala Cβ signal was observed in the NMR spectrum at a stretching ratio of more than ×6, suggesting the generation of heterogeneous structure in the PLA region [15]. Moreover, this structural change could be simulated by the MD calculations of the peptide $AGGAGG(A)_{12}GGAGAG$ under tensile conditions. This indicates that MD calculations are very effective for clarifying the mechanism of the conformational change of *S.c. ricini* silk fibroin [15].

In this paper, in order to elucidate the mechanism of the silk fiber formation in *S.c. ricini* silkworms, we reconstructed the three-dimensional architecture of silkworm spinneret from approximately 1000 optical micrographs of the semi-thin cross sections. We show that the silk press part is also important in the process of fiber formation. Finally, the molecular dynamics (MD) calculations were performed to study the details of the structural change which occur in the crystalline region of *S.c. ricini* silk fibroin under strong shear stress in detail.

2. Experimental part

2.1. Sample preparation

S.c. ricini silkworms were reared on an artificial diet in our laboratory. For serial sectioning, the silk press of a 7-day-old fifth instar larva that had just started to spin was fixed in situ with a solution containing a final concentration of 5(w/w)% glutaraldehyde. The silk press was dissected out in this solution and left for 7 days at 4 °C before post-fixation in 1(w/v)% aqueous osmium tetroxide for 1 day after washing in 0.1 M phosphate buffer. After embedding in Epon, 1 μm serial sections were cut (about 1000 sections) on an ultramicrotome with a diamond knife and stained with aqueous 1(w/v)% toluidine blue in borax before examination and photomicrography with a light microscope (×10 objective).

2.2. Three-dimensional reconstruction

The three-dimensional architecture was reconstructed using a software, TRI/3D-VOL (RATOC System Engineering Co. Ltd, Tokyo) from approximately 1000 optical micrographs of semi-thin cross sections. The reconstruction was prepared by tracing the outlines of the lumen, chitinous plates, and nascent (incompletely formed) fibroin brins on the computer after bringing the images into registration.

2.3. Molecular dynamics calculation

The structural change of *S.c. ricini* silk fibroin was examined with molecular dynamics (MD) calculation. Details of the MD simulations are described previously [15]. Four $AGGAGG(A)_{12}GGAGAG$ chains in α-helix conformation were placed in a periodic boundary cell homogeneously by using the ''crystal cell'' module. The chains were embedded in 351 water molecules for the initial arrangement of an aqueous solution system, which corresponds to the concentration of silk fibroin in the middle silk gland (about 30(w/v)%). Fig. 1 shows the initial structures of these model peptides used for MD simulation, where water molecules are also included. The Parrinello and Rahman method [20] was used for the MD calculation, where stress was applied by setting σ_{zz} (tensile stress) or σ_{xx} and σ_{yy} (shear stress) as non-zero value(s). The temperature of the system was controlled by the Andersen method at 298 K [21]. Both tensile and shear stresses were applied to the system. However, in order to emphasize the effect of the shear stress on the structural change of silk fibroin, the shear stress was changed from 0.1, 0.5, 1.0, 1.5 to 2.0 GPa under a tensile stress of 0.1 GPa. The steps of MD calculations are as follows. Initial calculations were performed without any external forces until the system reaches an equilibrium state (equilibrium stage; 5000 steps). From here the calculations continued under a tensile stress of 0.1 GPa (simulation stage; 200 000 steps, that is, 200 ps). A set of 100 structures were

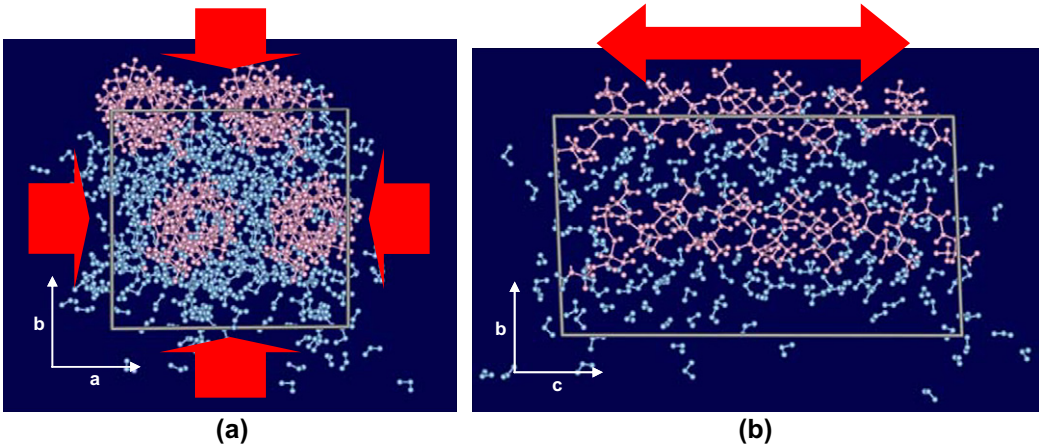

Fig. 1. Initial structures of the model peptide, AGGAGG(A)$_{12}$GGAGAG chains (pink) in an α-helix conformation for MD simulation. The water molecules (blue) are included. The directions of the shear stress (a) and tensile stress (b) applied to the system are shown as red arrows. (For interpretation of the references to colour in this figure legend, the reader is referred to the web version of this article)

sampled every 1000 steps during the latter stages of the simulation from 101 to 200 ps under various shear stresses and a tensile stress of 0.1 GPa in the presence of water. Finally, molecular mechanics (MM) calculations were performed after removal of water molecules. All the MD and MM simulations were carried out by using Discover 3 module in Insight II (4.0.0 P+, Accelrys Inc.) on OCTANE workstation (Silicon Graphics Inc.).

2.4. Conformational probability distribution

The conformational probability distributions of the Ala residues in the AGGAGG(A)$_{12}$GGAGAG chains were calculated at the equilibrium stage and after the MD calculations under external forces. Backbone torsion angles of the Ala residue, Ala (ϕ, ψ), were extracted from the trajectory of each simulation and used for the calculation of conformations $N(\phi \pm 10^\circ, \psi \pm 10^\circ)$. Here, $N(\phi \pm 10^\circ, \psi \pm 10^\circ)$ means the number of conformers with torsion angles: $(\phi \pm 10^\circ, \psi \pm 10^\circ)$. The conformational probability $P(\phi, \psi)$ of the Ala residues was calculated according to the following equation [22]:

$$P(\phi,\psi) = \frac{N\left(\phi \pm 10^{\circ}, \psi \pm 10^{\circ}\right)}{N_{\text{total}}}$$

where, N_{total} means total number of conformations of the Ala residues in the trajectory. The conformational probabilities $P(\phi, \psi)$ were plotted against the torsion angles, ϕ and ψ.

3. Results and discussion

3.1. Structure of the spinning apparatus in a wild silkworm S.c. ricini

Fig. 2a shows the optical micrographs of selected cross sections of the spinning apparatus of *S.c. ricini* silkworm and Fig. 2b shows the three-dimensional reconstruction obtained from approximately 1000 cross sections. The distal ends of the two silk gland ducts join to give a common tube 40 μm long with a wide lumen which, in turn, opens into the lumen of the silk press part. The nascent silk brins have evidently already drawn down before reaching the common tube according to the micrograph of cross section at 670 μm (the red arrow as shown in Fig. 2a). The cuticle lining of the silk press is thickened and is lip-shaped in the transverse section. Its lumen is flattened dorso-ventrally and bow-shaped. The shape of the lumen appears to be partly defined by one chitin plate in the cuticle lining close to the edge of the lumen (the white arrow at the micrograph of 450 μm in Fig. 2a), while there are two chitinous in the spinning apparatus of *B. mori* silkworm: one large ventral plate and a much narrower but much longer dorsal plate [23]. The start of chitin plate and the finish of plate define the length (230 μm) of the silk press proper. The plate did not cut well and is, therefore, probably quite hard. Moreover, from the finish of the spinning tube at around 330–400 μm, two left and right dorsal muscles have been observed on the cuticle of the silk press (yellow arrows in Fig. 2a) and run dorsally to insert on the cuticle of the head capsule. The muscles are thought to regulate the diameter and volume of the lumen of the silk press through their cooperated movement with the chitin plate to apply different tensile and shear stresses on the silk fibroin. The flexible cuticle at the corners of the lip-shaped cuticle may act as spring-loaded hinges allowing the press to return to the substantially closed position when the muscles relax so that the lumen of the silk press part appears to mold the fibroin filaments into a cross-sectional shape similar to those of the fully formed brins.

Fig. 3 shows the change in the cross sections of spinning apparatus tube-wall and lumen with the distance from its start at the spigot. In the spinning tube, the cross section of tube-wall is around 2000–4000 μm^2, which is increased gradually at the end of this part due to the appearance of muscles. The cross section showed a rapid increase in the silk press part and then fell slowly in the common tube (Fig. 3a). On the other hand, no significant cross section change was observed on the lumen till the end of silk press part, where the cross

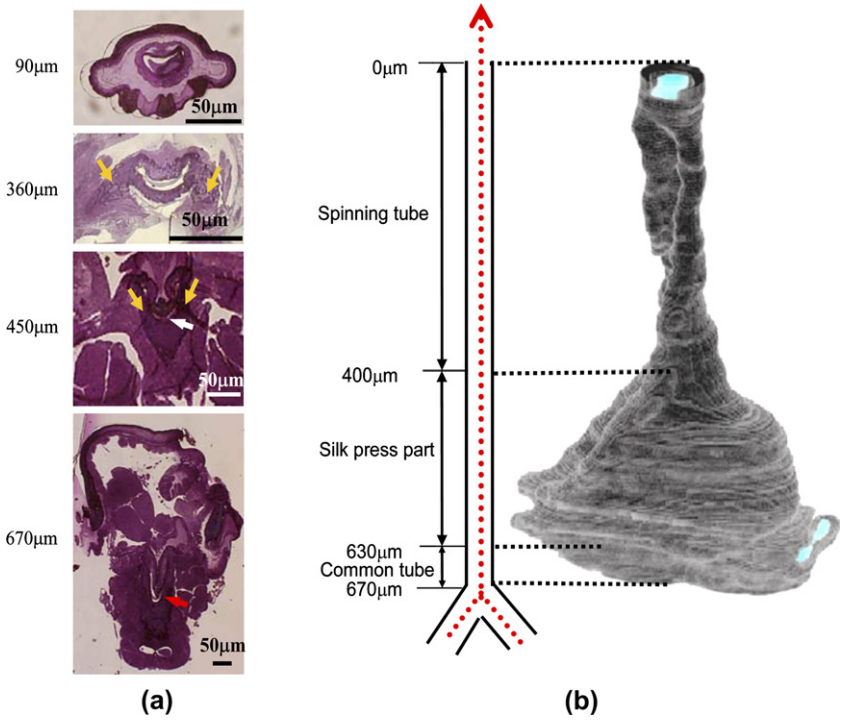

Fig. 2. (a) Optical micrographs of the cross sections of a spinneret. The nascent silk brin (red arrow), chitin plate (white arrow) and muscles (yellow arrows) are shown. (b) The three-dimensional reconstructed structure of the spinneret obtained from approximately 1000 optical micrographs of the cross sections of a spinneret using the software, TRI/3D-VOL. (For interpretation of the references to colour in this figure legend, the reader is referred to the web version of this article)

section was constant at about 500 μm^2. A slow increase and then a rapid initial increase appeared at the end of silk press part to the common tube (Fig. 3b). The progressive narrowing of the silkworm's lumen may help to prevent premature silk II formation as the fibroin flows through the duct during spinning by maintaining a low and fairly constant extensional flow. Thus the initial, rapidly converging part of the duct would, as in the spider, provide a slow linear movement of the fibroin solution along the duct and hence a long retention time for treating the fibroin with ions in this part of the duct [24].

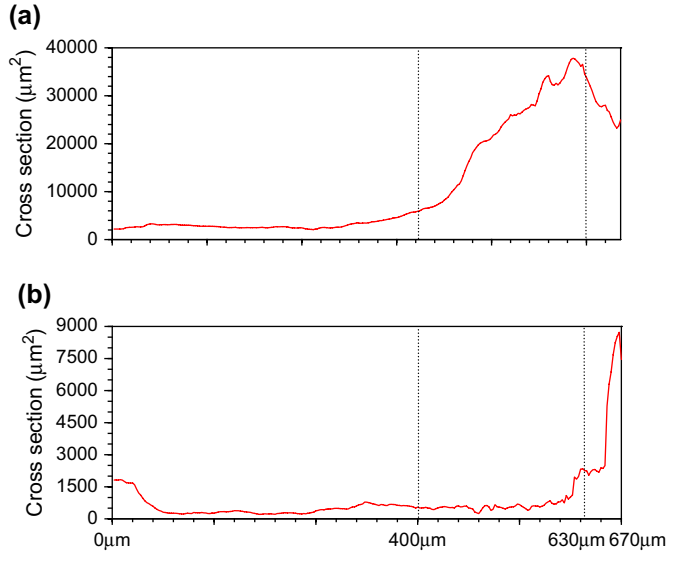

Fig. 3. Changes in the cross section(s) volumes (μm^2) of (a) the tube-wall and (b) lumen of the spinnerets of *S.c. ricini* silkworm vs. the distance from its start of spigot.

3.2. MD calculation of structural change in the PLA region of S.c. ricini

The structural change of *S.c. ricini* silk fibroin film induced by stretching could be well interpreted from the MD calculation of the peptide $AGGAGG(A)_{12}GGAGAG$ by including tensile stresses. This indicates that MD calculations can simulate the conformational change for the study of the structural transition of *S.c. ricini* silk fibroin [15]. Furthermore, previous studies prove that MD calculations were very effective in clarifying the mechanism of the conformational change as shown in *B. mori* silk fibroin previously [25,26]. In this work, we applied the MD calculation to study the structural transition of *S.c. ricini* silk fibroin based on the model peptide $AGGAG(A)_{12}GGAGAG$ under strong shear stress. Four $AGGAG(A)_{12}GGAGAG$ chains were placed in a periodic boundary cell homogeneously and the chains embedded in 351 water molecules for the initial arrangement of an aqueous solution system (Fig. 1). The conformation at Ala residues did not change under the tensile stress of 0.1 GPa and the α-helix, i.e. $(\phi, \psi) = (-60°, -60°)$ was the dominant conformation. So, the MD calculations in this work were performed by changing the shear stress while the tensile stress was fixed at 0.1 GPa because of the presence of a strong shear stress applied to the silk fibroin at the press part of the spinneret as described above.

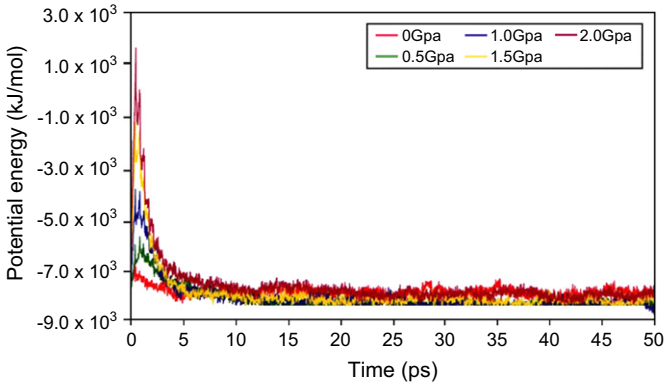

Fig. 4. Time course of the potential energies under a tensile stress at 0.1 GPa and shear stresses at 0, 0.5, 1.0, 1.5 and 2.0 GPa, respectively.

Fig. 4 is the time course of the potential energy under a tensile stress of 0.1 GPa and shear stresses of 0, 0.1, 0.5, 1.0, 1.5 and 2.0 GPa, respectively. Initially, each case showed unstable characteristics, which became stable and reached an equilibrium state after 5 ps from application of the shear stress. Fig. 5 shows the Ramachandran maps of conformational probability distributions of Ala residues from 80 to 100 ps under the tensile stress of 0.1 GPa and the shear stresses of 0, 0.1, 0.5, 1.0, 1.5 and 2.0 GPa, respectively, while still embedded in the water molecule environment. The conformation of the Ala residues was mainly α-helix, α_R (ϕ, ψ) = (−60°, −60°) under the tensile stress of 0.1 GPa without any shear stress (Fig. 5a). With increase in shear stress, several conformations, e.g., P_{II} (ϕ, ψ) = (−60°, 130°), α_R-like (ϕ, ψ) = (−150°, −60°), $C7^{ax}$ (ϕ, ψ) = (60°, −70°) and C_5 (ϕ, ψ) = (−150°, 150°) appeared and the C_5 became the dominant conformation when the shear stress was 1.0 GPa or more (Fig. 5b–f). This result suggested that the β-sheet formation could be induced and promoted after applying shear stress. Fig. 6 shows the average distance between Ala^1–N and Ala^{11}–N from 80 to

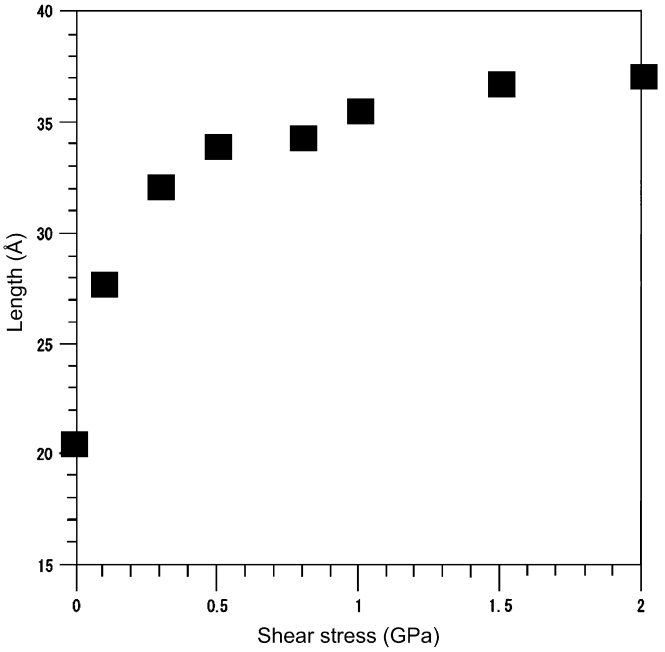

Fig. 6. Relationship between the molecular length and the shear stress from 80 to 100 ps under a tensile stress of 0.1 GPa. The molecular length is defined by the distance between Ala^1–N and Ala^{11}–N.

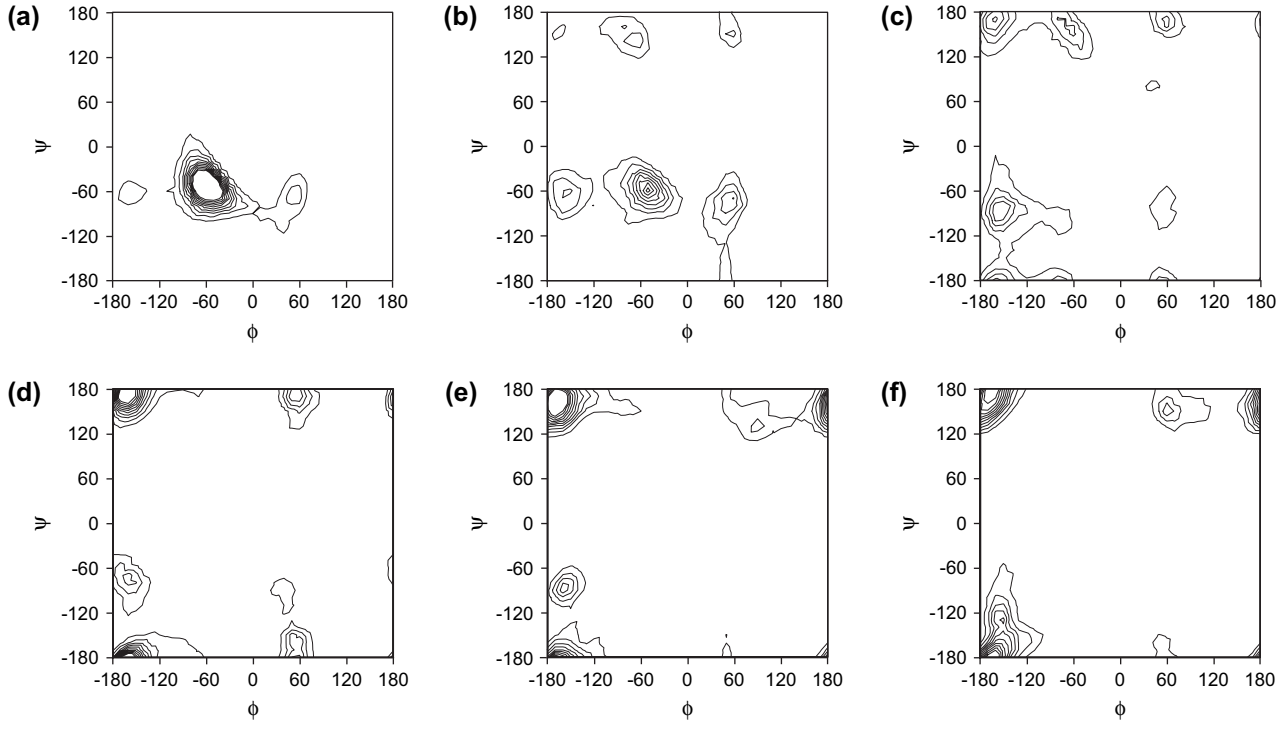

Fig. 5. Conformational probability maps of the Ala residues in the model peptide, $AGGAGG(A)_{12}GGAGAG$ in the presence of water molecules from 80 to 100 ps under a tensile stress of 0.1 GPa and shear stresses of (a) 0 GPa, (b) 0.1 GPa, (c) 0.5 GPa, (d) 1.0 GPa, (e) 1.5 GPa and (f) 2.0 GPa.

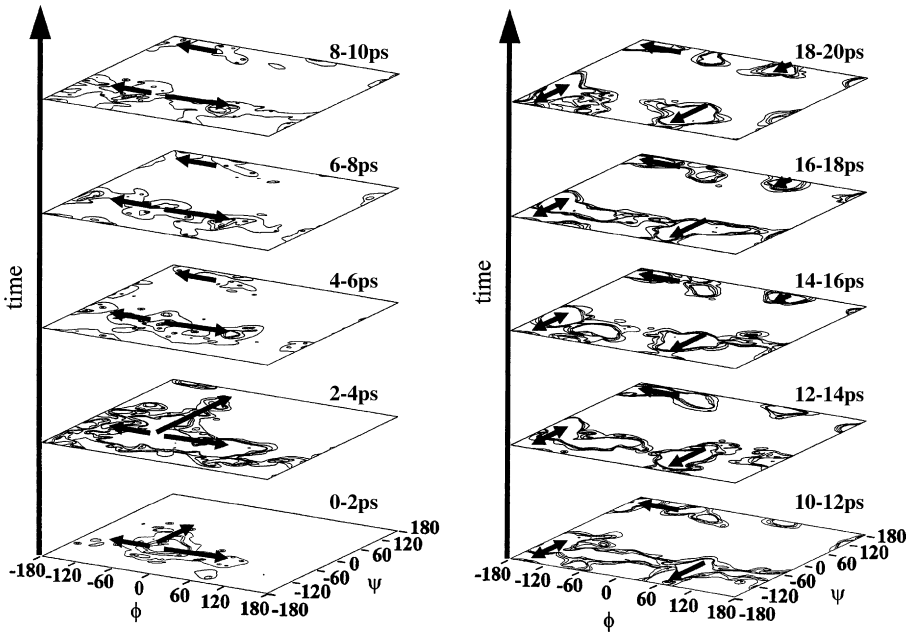

Fig. 7. Change in the conformational probability distributions of Ala residues in the model peptide, AGGAGG$(A)_{12}$GGAGAG in the presence of water molecules for every 2 ps from 0 to 20 ps, where 1.0 GPa of shear stress and 0.1 GPa of tensile stress were applied. (For interpretation of the references to colour in this figure legend, the reader is referred to the web version of this article)

100 ps under the tensile stress of 0.1 GPa and different shear stresses. At a shear stress of 1.0 GPa, the distance was around 35 Å, which is in agreement with PLA in a β-sheet structure.

Next, the time dependence of structural transition in PLA region was examined. Fig. 7 shows the change of conformational probability distribution every 2 ps for Ala residues in the aqueous solution system, where 1.0 GPa of shear stress and 0.1 GPa of tensile stress were applied, respectively. There are two different structural transition routes from α-helix to β-sheet structure: Type I is the $\alpha_R \rightarrow P_{II}$-like $\rightarrow C_5$ route (blue arrows in Fig. 7) and type II $\alpha_R \rightarrow \alpha_R$-like $\rightarrow C_5$ (red arrows in Fig. 7). Since the C_5 conformation becomes the dominant conformation at a shear stress of 1.0 GPa and above in the presence of water molecules as shown in Fig. 5d–f, the water molecules were then removed and MM calculations were performed by taking into account the fact that the water molecules are rapidly evaporated just after the spinning by the *S.c. ricini* silkworm. After the removal of water molecules the change in the Ramachandran map of Ala residues is remarkable as shown in Fig. 8a–c, where the P_{II}-like (−100°, 130°) conformation appeared. This structural change is speculated to be due to new hydrogen bond formation between peptide chains after the breaking of hydrogen bonds between the peptide chains and water molecules.

4. Conclusions

From the reconstruction of three-dimensional architecture of silkworm spinneret from approximately 1000 optical micrographs of the semi-thin cross sections, our observations may contribute to a further understanding of the natural spinning process in *S.c. ricini* silkworm. The MD simulation was then

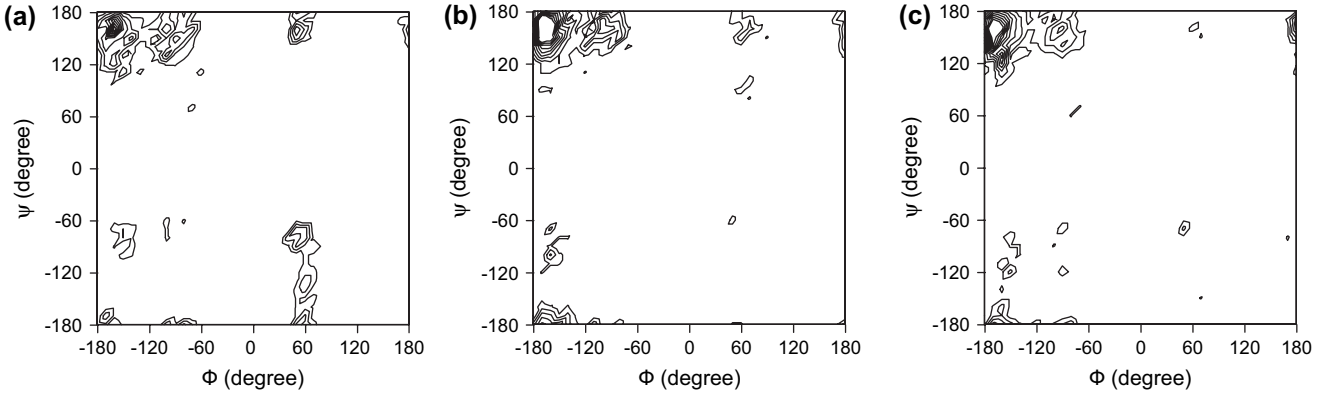

Fig. 8. Conformational probability maps of Ala residues in the model peptide, AGGAGG$(A)_{12}$GGAGAG from 80 to 100 ps under a tensile stress of 0.1 GPa and share stresses of (a) 1.0 GPa, (b) 1.5 GPa and (c) 2.0 GPa, after the water molecules were removed.

performed to study the structural change which occur in the crystalline region of silk fibroin under strong shear stresses by mimicking the silk press part in the silkworm spinneret in the presence of water molecules and then MM calculation after removal of water molecules.

Acknowledgements

TA acknowledges Dr. Tsutomu Yamane for technical support in the MD simulations, and also grant support from the Insect Technology Project, Japan and the Agriculture Biotechnology Project, Japan. JY acknowledges support from the National Natural Science Foundation of China (No. 20404011) and Zhejiang Natural Science Foundation of China (No. R404066).

References

[1] Asakura T, Kaplan DL. In: Arutzen CJ, editor. Encyclopedia of agricultural science, vol. 4. New York: Academic Press; 1994. p. 1–11.
[2] Yao JM, Asakura T. In: Wnek GE, Bowlin GL, editors. Encyclopedia of biomaterials and biomedical engineering. New York: Marcel Dekker, Inc.; 2004. p. 1363–70.
[3] Altman GH, Diaz F, Jakuba C, Calabro T, Horan RL, Chen J, et al. Biomaterials 2003;24:401–16.
[4] Cappello J, Ferrari F. In: Mobley DP, editor. Plastics from microbes. New York: Hanser; 1994. p. 35–92.
[5] Lazaris A, Arcidiacono S, Huang Y, Zhou J, Duguay F, Chretien N, et al. Science 2002;295:472–6.
[6] Yao J, Asakura T. J Biochem 2003;133:147–54.
[7] Yukuhiro K. Personal communication.
[8] Xu M, Lewis RV. Proc Natl Acad Sci USA 1990;87:7120–4.
[9] Sponner A, Schlott B, Vollrath F, Unger E, Grosse F, Weisshart K. Biochemistry 2005;44:4727–36.
[10] Hinman MB, Lewis RV. J Biol Chem 1992;267:19320–4.
[11] Nakazawa Y, Bamba M, Nishio S, Asakura T. Protein Sci 2003;12:666–71.
[12] Nakazawa Y, Asakura T. FEBS Lett 2002;529(2–3):188–92.
[13] Nakazawa Y, Nakai T, Kameda T, Asakura T. Chem Phys Lett 1999;311:362–6.
[14] Van Beek JD, Beaulieu L, Schafer H, Demura M, Asakura T, Meier BH. Nature 2000;405:1077–9.
[15] Nakazawa Y, Asakura T. J Am Chem Soc 2003;125:7230–7.
[16] Yang M, Yao J, Sonoyama M, Asakura T. Macromolecules 2004;37:3497–504.
[17] Magoshi J, Magoshi Y, Nakamura S. J Appl Polym Sci Appl Polym Symp 1985;41:187–204.
[18] Kataoka K, Umatsu I. Kobunshi Ronbunshu 1977;34:37–41.
[19] Ogiwara S. Kensi-no-Kouzou. Japan: Shinshu University; 1957. p. 20–45.
[20] Parrinello M, Rahman A. J Appl Phys 1981;52:7182–90.
[21] Andersen HC. J Chem Phys 1980;72:2384–93.
[22] Yamane T, Inoue Y, Sakurai M. Chem Phys Lett 1998;291:137–42.
[23] Asakura T, Umemura K, Nakazawa Y, Hirose H, Higham J, Knight D. Biomacromolecules 2007;8:171–81.
[24] Vollrath F, Knight D. Nature 2001;410:541–8.
[25] Yamane T, Umemura K, Nakazawa Y, Asakura T. Macromolecules 2003;36:6766–72.
[26] Yao J, Nakazawa Y, Asakura T. Biomacromolecules 2004;5:680–8.